

Synthesis and Design of 5G Duplexer Based on Optimization Method



WU Qingqiang¹, CHEN Jianzhong¹, WU Zengqiang²,
GONG Hongwei²

(1. National Key Laboratory of Antennas and Microwave Technology, Shaanxi Joint key Laboratory of Graphene, Xidian University, Xi'an 710071, China;

2. ZTE Corporation, Shenzhen 518057, China)

DOI: 10.12142/ZTECOM.202203009

<https://kns.cnki.net/kcms/detail/34.1294.TN.20220712.1122.002.html>,
published online July 12, 2022

Manuscript received: 2021-10-21

Abstract: A new optimization method is proposed to realize the synthesis of duplexers. The traditional optimization method takes all the variables of the duplexer into account, resulting in too many variables to be optimized when the order of the duplexer is too high, so it is not easy to fall into the local solution. In order to solve this problem, a new optimization strategy is proposed in this paper, that is, two-channel filters are optimized separately, which can reduce the number of optimization variables and greatly reduce the probability of results falling into local solutions. The optimization method combines the self-adaptive differential evolution algorithm (SADE) with the Levenberg-Marquardt (LM) algorithm to get a global solution more easily and accelerate the optimization speed. To verify its practical value, we design a 5G duplexer based on the proposed method. The duplexer has a large external coupling, and how to achieve a feed structure with a large coupling bandwidth at the source is also discussed. The experimental results show that the proposed optimization method can realize the synthesis of higher-order duplexers compared with the traditional methods.

Keywords: optimization; self-adaptive differential evolution algorithm; LM optimization algorithm; filter synthesis; duplexer

Citation (IEEE Format): Q. Q. Wu, J. Z. Chen, Z. Q. Wu, et al, "Synthesis and design of 5G duplexer based on optimization method," *ZTE Communications*, vol. 20, no. 3, pp. 70 - 76, Sept. 2022. doi: 10.12142/ZTECOM.202203009.

1 Introduction

With the rapid development of the 5G technology, microwave duplexers have been widely used in wireless and satellite communications. The earliest method of synthesizing duplexers was connecting two channel filters directly to a common cavity, and then modifying the parameters of each filter to compensate for the interaction between the two channels^[1-2]. This method was limited by the number of channels and the coupling topology of the channel filter, and the synthesis results would get worse as the frequency band approaches.

In recent years, MACCHIARELLA and TAMIAZZO have proposed a more efficient and flexible method for synthesizing duplexers^[3]. In this method, the transmission function and reflection function of each channel filter are derived from the relationship between the global parameters of the duplexer and the parameters of the independent channel filter. Recently, ZHAO Ping and WU Keli proposed a new duplexer synthesis method^[4-6], by which all the channel filters are synthesized

separately under the consideration of the influence of other channels and the process is repeated to ensure that the final results meet the requirements.

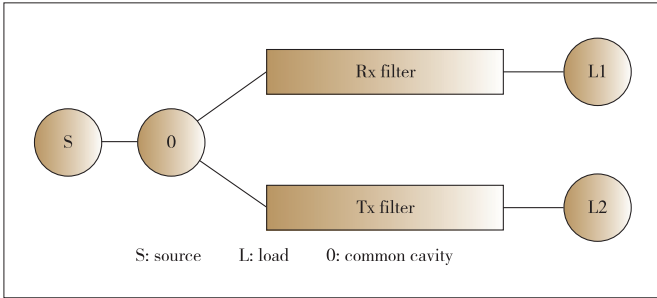
In this paper, the self-adaptive differential evolution algorithm^[7-8] and the LM optimization algorithm^[9-10] are used instead of the analytical method to obtain the coupling matrix of a single channel filter. The self-adaptive differential evolution algorithm can reduce the probability of convergence to local solutions while the LM method can improve the optimization speed. Compared with the analytical methods mentioned above, an optimization algorithm has a higher degree of freedom, and the optimization algorithm proposed in this paper can achieve a higher order than the traditional optimization algorithm. Because the optimized duplexer requires a larger coupling structure between the source and the common cavity, how to achieve a larger port coupling is also discussed in this paper.

2 Design of Duplexer Optimization Algorithm

Fig. 1 illustrates the structure of the star-junction duplexer, which consists of two filters connected in parallel to the same common cavity. The parameters S, L1, and L2 in the figure represent the source and load of the duplexer, while 0 repre-

This work was supported by the National Natural Science Foundation of China (NSFC) under project no. 62071357 and the Fundamental Research Funds for the Central Universities.

sents the common cavity. Before the duplexer optimization, the transmission and reflection polynomials of a single channel filter should be obtained by the traditional generalized Chebyshev synthesis method^[11], and then we need to transform the polynomials of these filters so that they correspond to the passband of the duplexer. Finally, the corresponding coupling matrix is extracted according to the polynomial after transformation, which is taken as the initial value of optimization. The source and the common cavity are generally 1.4 according to experience.



▲ Figure 1. Structure of star-junction duplexer

As a global optimization algorithm, the adaptive differential evolution algorithm needs to determine the upper and lower limits of the variables to be optimized according to the initial values in order to improve the optimization speed and success rate. Since the influence of other channels is mainly reflected in the first cavity of the filter, the upper and lower limits of the coupling between the source and the common cavity are taken as “initial value ± 0.1 ”, and the limits of the coupling between the common cavity and the first cavity of two channels are taken as “initial value ± 0.2 ”. In addition, the self-coupling of the first cavity of each channel are taken as “initial value ± 0.2 ” as well. Finally, the limits of the rest couplings are taken as “initial value ± 0.05 ”. The advantages of the adaptive differential evolution algorithm are as follows. 1) An adaptive control mechanism is adopted for parameters in optimization; 2) In order to avoid falling into the local solution, a new operator, called the self-adaptive return operator, is activated when the optimization is judged to be trapped in local optima, which can often be observed in earlier iterations if it happens. That is the algorithm searches again according to the initial value and its range, when trapped in a local solution.

After the upper and lower limits of the optimized variables are obtained, it is the choice of the objective function, which also plays a key role in the success of optimization. For coupling matrix synthesis, the objective function is formed by S-parameter specifications which can be calculated according to Eqs. (1) and (2). In this paper, the objective function of optimizing a single channel filter for the first time is given in Eq. (3). When optimizing another channel filter, its objective function is given in Eq. (4).

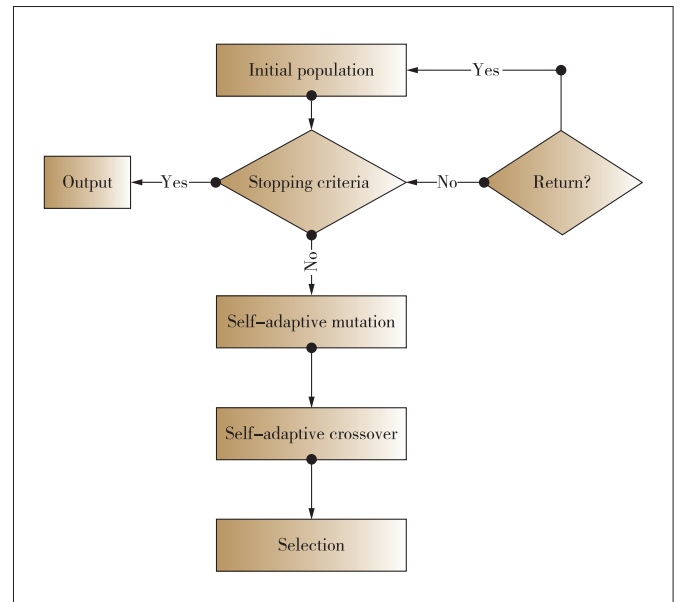
$$S_{pp} = \pm \left(1 - 2[A]_{pp}^{-1} \right), \quad (1)$$

$$S_{pq}|_{p \neq q} = 2[A]_{pq}^{-1}. \quad (2)$$

$$f(x) = \frac{|\max[S_{11}(\text{PB}_1)] - \text{RL}|}{|\text{RL}|} + \frac{|\max[S_{21} - \text{Attenu}]|}{|\text{Attenu}|}, \quad (3)$$

$$f(x) = \frac{|\max[S_{11}(\text{PB}_1)] - \text{RL}|}{|\text{RL}|} + \frac{|\max[S_{11}(\text{PB}_2)] - \text{RL}|}{|\text{RL}|} + \frac{|\max[S_{21} - \text{Attenu}]|}{|\text{Attenu}|} + \frac{|\max[S_{31} - \text{Attenu}]|}{|\text{Attenu}|}. \quad (4)$$

Among them, PB_k denotes the k -th ($k = 1, 2$) passband. Return loss (RL) and Attenu are the desired return loss and restraint outside the band, respectively. Fig. 2 shows the general steps of the adaptive differential evolution algorithm.



▲ Figure 2. Flow diagram of the adaptive differential evolution algorithm

After the approximate response curve is obtained by the adaptive differential evolution algorithm, the LM algorithm is adopted in the optimization algorithm, and the reflection zero, passband edge return loss, and transmission zero of the corre-

sponding channel filter are selected as the sampling points. In summary, the basic steps of the algorithm can be obtained as follows, and the algorithm is realized by Matlab^[12].

1) Initial selection. According to the requirements of the index, the transmission and reflection polynomials of the two-channel filters are obtained by using the generalized Chebyshev synthesis method, then the corresponding duplexer polynomials are obtained by frequency transformation, and the initial values of the optimized variables are obtained after the coupling matrix is extracted and rotated. The variables to be optimized include the coupling M_{s0} between source and common cavities, the mutual coupling M_{ij} ($i \neq j$) between cavities, and the self-coupling M_{ii} of cavities.

2) Determining the range of variables. According to the obtained initial value, we can define the value range of the corresponding variable. The specific method has been introduced and will not be repeated here.

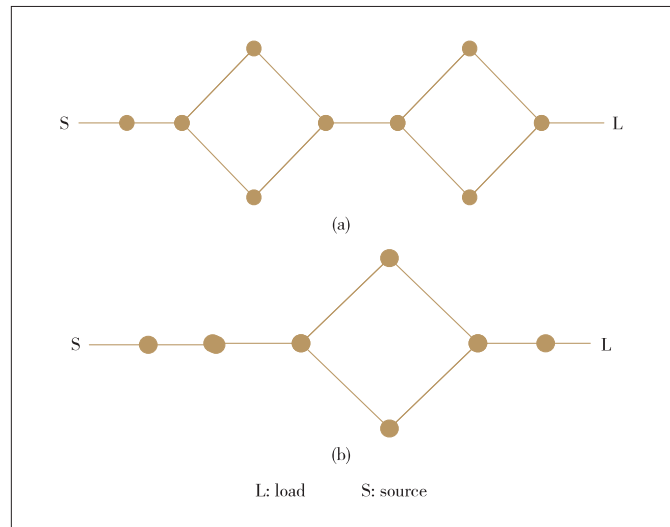
3) Optimization of the low-frequency channel filter. The coupling between the source and the common cavity and the non-zero elements of the low-frequency channel filter coupling matrix is selected as optimization variables, and the elements of the high-frequency channel filter coupling matrix are kept unchanged. The differential evolution algorithm and Eq. (1) are used to optimize the low-frequency channel filter.

4) Optimization of the high-frequency channel filter. Similarly, the coupling between the source and the common cavity and the non-zero elements of the high-frequency channel filter coupling matrix is selected as optimization variables, and the elements of the low-frequency channel filter coupling matrix remain unchanged. The differential evolution algorithm and Eq. (2) are used to optimize the high-frequency channel filter.

5) Optimization of the coupling matrix of the duplexer with the LM algorithm. The duplexer model obtained by the differential evolution algorithm can meet the requirements of the index, but still there is room for optimization. LM algorithms as a gradient optimization algorithm can make the final frequency response better meet the requirements. Different from the adaptive differential evolution algorithm, the LM algorithm uses the reflection zeros of the two-channel filters, the points on the channel edge, and the transmission zeros as the sampling points.

3 Experiments and Results Discussion

To verify the above design, an example of a duplexer that has a low-frequency channel of order 9 and a high frequency channel of order 7 is used. Fig. 3 shows the specific topology of this duplexer and the following tables list the specifications of the duplexer (Table 1 shows the passband range and return loss and Table 2 shows the restraint outside the band). The parameters S and L in the figure represent the source and load of the filter respectively. The box topology in Fig. 3 is chosen mainly for the reason that the box topology is easier to realize



▲ Figure 3. Diplexer topology used in the example: (a) low frequency topology and (b) high frequency topology

▼ Table 1. Passband indicators

Passband Range/MHz	Return Loss/dB
1 710 - 1 785	-17
1 920 - 1 980	-17

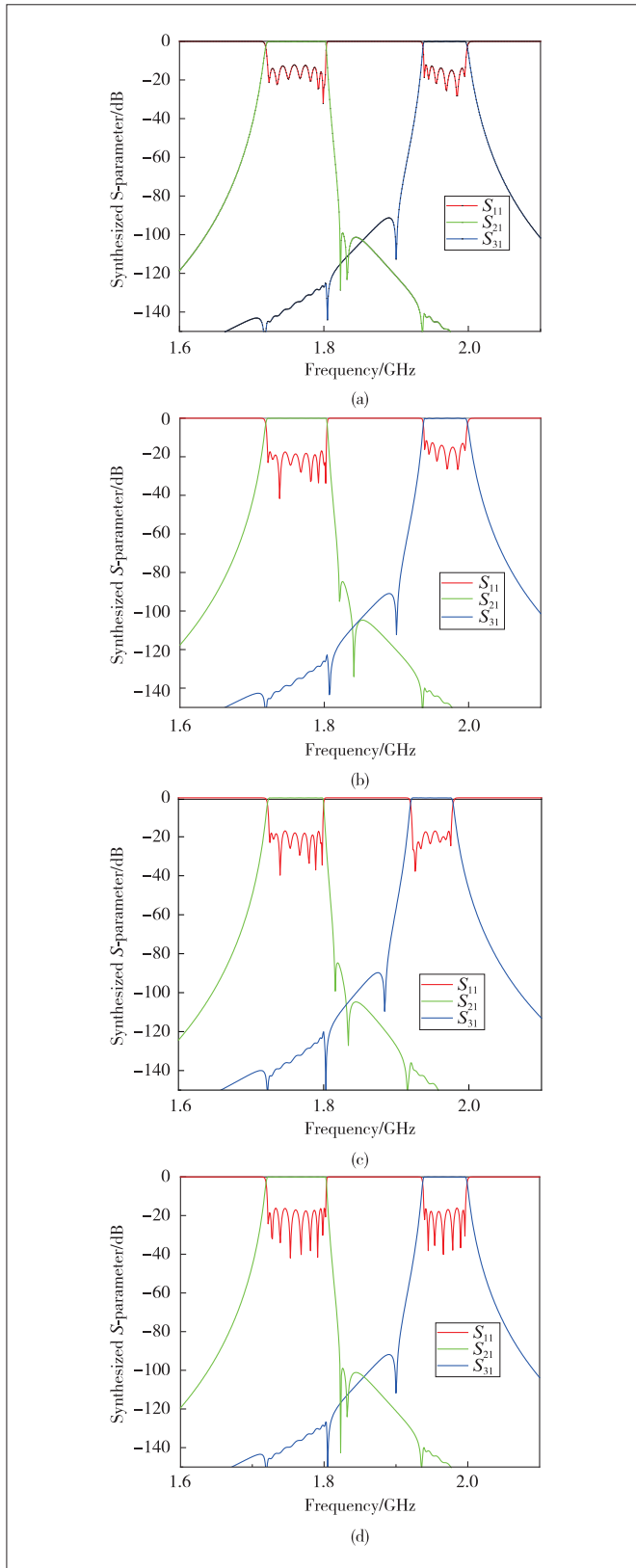
▼ Table 2. Restraint outside the band

Low-Frequency Channel Filter		High-Frequency Channel Filter	
1 805 - 1 880 MHz	-80 dB	1 805 - 1 880 MHz	-80 dB

in simulation and machining, and the parasitic influence between cavities can be reduced due to the lack of diagonal coupling. It can be seen that the passband range of the low-frequency channel filter is 1 710 - 1 785 MHz, the passband range of the high-frequency channel filter is 1 920 - 1 980 MHz, and the return loss in both passbands is -17 dB. Both of the two-channel filters require -80 dB out-of-band suppression in 1 805 - 1 880 MHz. To achieve this goal, two additional transmission zeros should be introduced for the low frequency channel filter and one transmission zero for the high frequency channel filter. How to use optimization algorithms to achieve these indicators will be described below.

First, we use the generalized Chebyshev synthesis method to get the initial value of the duplexer, and the corresponding response curve is shown in Fig. 4(a). It can be seen that due to the interaction between the two channels, the response in the passband of the duplexer becomes very poor.

After the initial value of the coupling variable of the duplexer is obtained, according to the above theory and experience, we can design the initial values of the variables and their optimization intervals. Then we keep the value of the high-frequency channel filter coupling matrix unchanged. According to Eq. (1) and the index requirements in Tables 1 and 2, we use the adaptive differential evolution algorithm to optimize the coupling variables of the low-frequency channel. The results of optimization are shown in Fig. 4(b), where the response in the



▲ Figure 4. (a) Initial response of the duplexer, (b) corresponding result after optimizing low channel filter in the first iteration, (c) corresponding result after optimizing high channel filter in the first iteration, and (d) final result

passband of the low-frequency channel filter has been greatly improved after optimization.

Similarly, we keep the value of the low-frequency channel filter coupling matrix unchanged. According to Eq. (2) and the index requirements in Tables 1 and 2, the adaptive differential evolution algorithm is used to optimize the coupling variables of the high-frequency channel. The results of optimization are shown in Fig. 4(c). It can be seen that although the final curve meets the requirements of the index, there is still room for optimization. We do gradient optimization on the final result to make it converge to the optimal solution. The optimization algorithm is the LM algorithm, and the sampling point is the reflection zero and transmission zero of the two channel filters. Fig. 4(d) shows that after gradient optimization, the final result curve further meets our requirements, and the values of the coupling matrix corresponding to each figure in Fig. 4 are listed in Table 3.

After the coupling matrix of the duplexer is obtained by the optimization algorithm, a simulation analysis is needed. Because the relative bandwidth of the duplexer is 14.67%, the coverage band is wide, the two passband bands of the duplexer are far apart, and the intermediate interval bandwidth accounts for 50% of the coverage band of the whole duplexer, which puts forward a great demand for the coupling bandwidth of the feed. According to the optimization results, the port needs to provide a coupling between the source and the common cavity of 1.391. According to Eq. (5), the required external Q value is 3.524. Under such requirements, it is difficult for the traditional coupling structure to achieve such a large coupling bandwidth for the duplexer realized by the dielectric waveguide. Therefore, before simulation, it is necessary to discuss how to realize the coupling structure design of the large coupling feed.

$$Q_e = \frac{1}{FBW \times M_{s0}^2} \quad (5)$$

In order to solve this problem, this paper introduces a new type of joint structure, the model of which is shown in Fig. 5. We can see that the whole is a dielectric waveguide cavity fed by coaxial taps. A cuboid groove is dug just below the tap, a through hole is used to connect the tap with the groove, and the through hole is covered with metal.

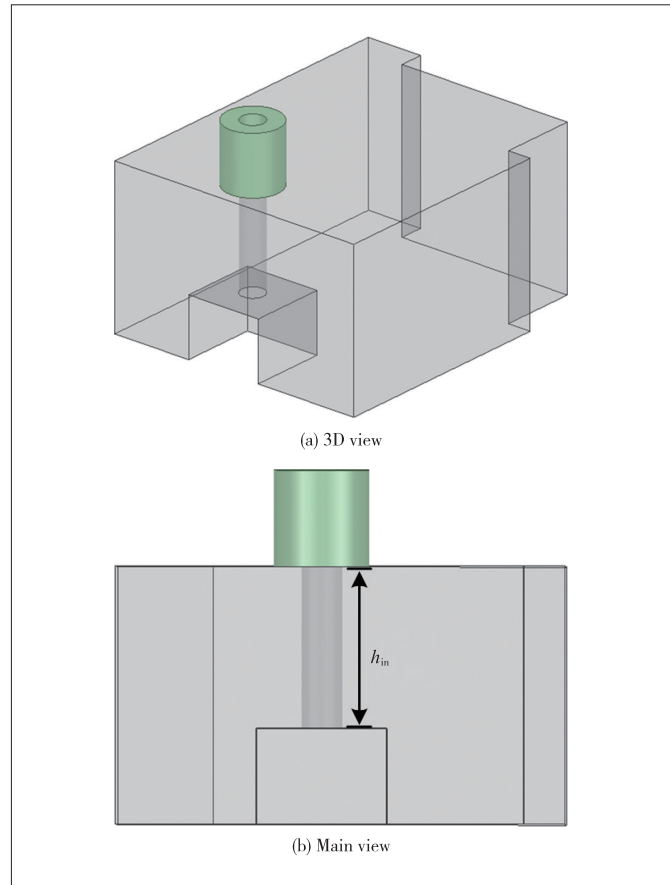
The cavity form from the groove to the tap becomes a quarter wavelength resonant unit. The metal-coated through hole in the inner wall is equivalent to the inner conductor of the coaxial resonant unit. The resonant frequency of the coaxial resonant unit can be adjusted by adjusting h_{in} . The resonant element is essentially the common cavity part of the common cavity type circuit structure, while the rest of the waveguide cavity is not necessary, which can be retained or not retained according to the overall model of the duplexer. Although eliminating redundant waveguide cavities can effectively reduce

▼Table 3. Values of the coupling matrix

	Initial	First	Second	Final
M(s,0)	1.400 0	1.388 4	1.374 2	1.391 0
M(0,1)	0.658 7	0.704 4	0.690 8	0.673 1
M(0,10)	0.658 7	0.644 9	0.651 8	0.584 2
M(9,L1)	0.501 3	0.517 4	0.517 4	0.501 3
M(16,L2)	0.427 2	0.427 2	0.428 7	0.427 2
M(1,1)	0.708 9	0.661 7	0.661 7	0.656 5
M(1,2)	0.225 4	0.224 5	0.224 5	0.211 1
M(2,2)	0.709 1	0.704 7	0.704 7	0.703 4
M(2,3)	0.092 4	0.091 3	0.091 3	0.092 4
M(2,4)	-0.139 8	-0.145 1	-0.145 1	-0.139 3
M(3,3)	0.490 6	0.478 2	0.478 2	0.489 8
M(3,5)	0.083 2	0.080 0	0.080 0	0.083 0
M(4,4)	0.805 4	0.798 5	0.798 5	0.804 0
M(4,5)	0.130 9	0.137 2	0.137 2	0.131 0
M(5,5)	0.712 8	0.715 2	0.715 2	0.712 5
M(5,6)	0.155 1	0.158 3	0.158 3	0.155 5
M(6,6)	0.714 1	0.717 4	0.717 4	0.714 0
M(6,7)	0.086 5	0.084 8	0.084 8	0.086 5
M(6,8)	0.132 2	0.139 3	0.139 3	0.132 1
M(7,7)	0.489 3	0.476 9	0.476 9	0.489 2
M(7,9)	-0.131 4	-0.133 2	-0.133 2	-0.132 0
M(8,8)	0.822 1	0.821 4	0.821 4	0.822 0
M(8,9)	0.183 1	0.190 8	0.190 8	0.183 2
M(9,9)	0.709 3	0.704 9	0.704 9	0.708 7
M(10,10)	-0.790 9	-0.790 9	-0.743 2	-0.748 4
M(10,11)	0.163 8	0.163 8	0.178 5	0.155 9
M(11,11)	-0.791 1	-0.791 1	-0.790 2	-0.787 7
M(11,12)	0.122 2	0.122 2	0.130 5	0.122 0
M(12,12)	-0.791 6	-0.791 6	-0.792 7	-0.790 8
M(12,13)	0.070 7	0.070 7	0.071 7	0.092 0
M(12,14)	-0.091 9	-0.091 9	-0.097 2	0.070 7
M(13,13)	-0.647 5	-0.647 5	-0.642 7	-0.647 3
M(13,15)	0.075 1	0.075 1	0.077 3	0.075 0
M(14,14)	-0.879 1	-0.879 1	-0.884 2	-0.878 9
M(14,15)	0.096 3	0.096 3	0.107 9	0.096 35
M(15,15)	-0.791 1	-0.791 1	-0.793 5	-0.791 0
M(15,16)	0.163 8	0.163 8	0.170 4	0.163 8
M(16,16)	-0.791 0	-0.791 0	-0.783 5	-0.790 8

the volume of the joint structure, in most cases, the coupling between the common cavity and the channel filter still needs to be realized by window coupling, and the physical connection between the joint structure and the channel filter can be realized by reserving the waveguide cavity.

In addition to the coupling between the source and the common cavity, the coupling bandwidth between the common cavity and the channel filter is also relatively high. Large inter-cavity coupling of waveguide cavities located in the same layer is easy to achieve by opening windows, but for duplexers

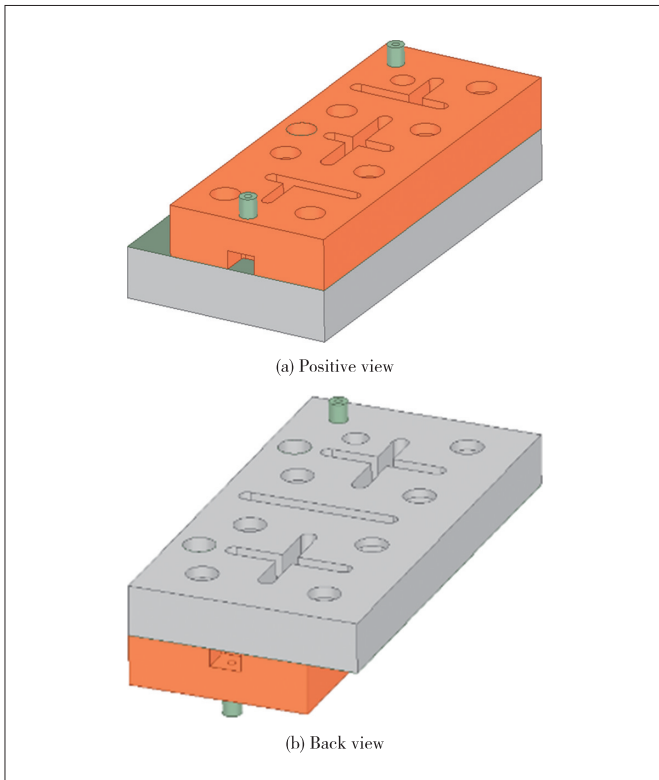


▲ Figure 5. Closed circuit structure model with large coupling

with more orders, placing all cavities in the same layer will lead to too much device area. Therefore, in practice, a two-layer structure is preferred.

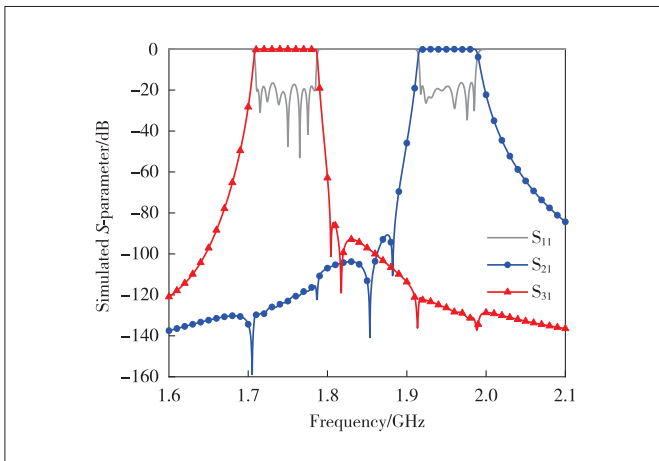
After the coupling structure of the feed part is obtained, the overall model of the duplexer is simulated as is shown in Fig. 6.

We can see that the waveguide duplexer is filled with ceramic, and the whole duplexer is divided into two layers, in which the joint structure is located in the first layer. In order to avoid this problem, the order of channel 1 is increased to 9 in this scheme. As shown in Fig. 6(a), the input port, namely the junction structure, is located at the window between the two cavities. Its left and right sides are the first cavity of channel 2 and the first cavity of channel 1 respectively. The coupling amount of the common cavity to the two channels can be adjusted by the size of the window and the relative position of the input port from the two ports in the horizontal direction. The cavities 2 - 7 of channel 2 are located in the first layer, and the cavities 2 - 9 of channel 1 are located in the second layer. The inter-cavity coupling between cavity 1 and cavity 2 in channel 1 requires a small coupling bandwidth, which is achieved by opening a circular window between layers. The simulation results of the model are shown in Fig. 7. The simulation results in Fig. 7 show that the design meets the require-



▲ Figure 6. Simulation model of double-layer duplexer

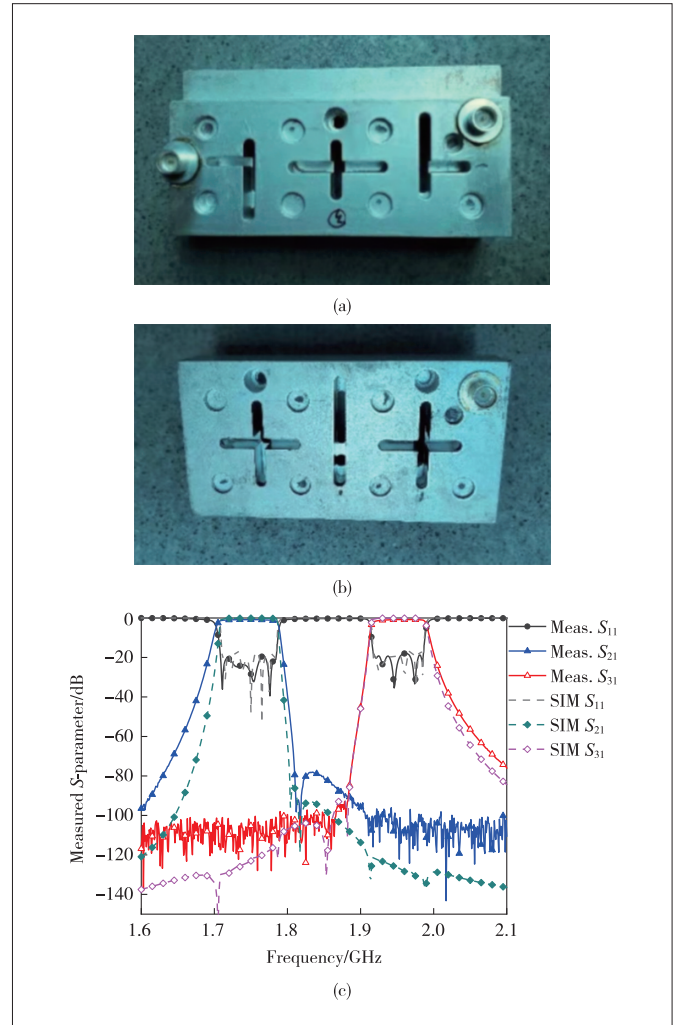
ments of the indicators.



▲ Figure 7. Electromagnetic simulation (EM) simulation results of the model

Finally, we made physical processing of the simulated model and measured the processed physical object. The finished product is shown in Figs. 8(a) and 8(b). The comparison between the frequency response results and the simulation results is shown in Fig. 8(c) and the optimization results we hope to obtain can be referred to in Fig. 4(d). Among them, the measured results of the duplexer are solid lines in the Fig. 8 (a), which meet the requirements of the index, and are basi-

cally consistent with the simulation results represented by dotted lines, which verifies the effectiveness of the algorithm and the circuit combination structure proposed in this paper.



▲ Figure 8. (a) Positive view, (b) back view, and (c) comparison between the measured results and the simulation results

4 Conclusions

In this paper, a star junction duplexer synthesis method based on the adaptive differential evolution algorithm (SADE) and LM optimization algorithm is proposed. As a global optimization algorithm, the adaptive differential evolution algorithm can effectively avoid the convergence of optimization results to local solutions, while the LM algorithm as a gradient optimization algorithm can not only accelerate the optimization speed, but also make the results more in line with the requirements of the index. In order to verify the effectiveness of the algorithm, a duplexer with large port coupling is designed, and the structure of realizing large port coupling is also given in this paper.

References

- [1] RHODES J D, LEVY R. A generalized multiplexer theory [J]. IEEE transactions on microwave theory and techniques, 1979, 27(2): 99 - 111. DOI: 10.1109/tmtt.1979.1129570
- [2] RHODES J D, LEVY R. Design of general manifold multiplexers [J]. IEEE transactions on microwave theory and techniques, 1979, 27(2): 111 - 123. DOI: 10.1109/tmtt.1979.1129571
- [3] MACCHIARELLA G, TAMIAZZO S. Novel approach to the synthesis of microwave duplexers [J]. IEEE transactions on microwave theory and techniques, 2006, 54(12): 4281 - 4290. DOI: 10.1109/TMTT.2006.885909
- [4] MENG H, WU K L. Direct optimal synthesis of a microwave bandpass filter with general loading effect [J]. IEEE transactions on microwave theory and techniques, 2013, 61(7): 2566 - 2573. DOI: 10.1109/TMTT.2013.2264682
- [5] ZHAO P, WU K L. An analytical approach to synthesis of duplexers with an optimal lumped-element junction model [C]//2014 IEEE MTT-S international microwave symposium (IMS2014). IEEE, 2014: 1 - 3. DOI: 10.1109/MWSYM.2014.6848399
- [6] ZHAO P, WU K L. An iterative and analytical approach to optimal synthesis of a multiplexer with a star-junction [J]. IEEE transactions on microwave theory and techniques, 2014, 62(12): 3362 - 3369. DOI: 10.1109/TMTT.2014.2364222
- [7] LIU B, YANG H, LANCASTER M J. Synthesis of coupling matrix for duplexers based on a self-adaptive differential evolution algorithm [J]. IEEE transactions on microwave theory and techniques, 2018, 66(2): 813 - 821. DOI: 10.1109/tmtt.2017.2772855Jan. 2018.
- [8] YU Y, LIU B, WANG Y, et al. A general coupling matrix synthesis method for all-resonator duplexers and multiplexers [J]. IEEE transactions on microwave theory and techniques, 2020, 68(3): 987 - 999. DOI: 10.1109/TMTT.2019.2957430
- [9] SKAIK T F, LANCASTER M J, HUANG F. Synthesis of multiple output coupled resonator circuits using coupling matrix optimisation [J]. IET microwaves, antennas & propagation, 2011, 5(9): 1081. DOI: 10.1049/iet-map.2010.0447
- [10] XIA W L. Duplexers and multiplexers design by using coupling matrix optimization [D]. Birmingham, U.K.: Birmingham University, 2015
- [11] CAMERON R J, KUDSIA C M, MANSOUR R R. Microwave filters for communication systems [M]. Hoboken, USA: John Wiley & Sons, Inc., 2018. DOI: 10.1002/9781119292371
- [12] MATLAB. MATLAB optimization toolbox. user's guide [EB/OL]. (2018-05-12) [2021-09-18]. <https://www.mathworks.com>

Biographies

WU Qingqiang received his BS degree in electromagnetic field and wireless technology and MS degree in electronic science and technology from Xidian University, China in 2019 and 2022, respectively. He joined ZTE Corporation in 2022 after graduation. During his postgraduate study, he mainly engaged in the research related to filters in the National Key Laboratory of Antennas and Microwave Technology at Xidian University, and participated in the publication of papers in academic journals and international conferences and completed a number of filter related projects. In addition, he won the first-class scholarship of the university for many times, and won the second prize of northwest division in the 15th China Graduate Electronic Design Competition.

CHEN Jianzhong (jianzhong.chen@xidian.edu.cn) received his BE degree in information engineering from Xi'an Jiaotong University, China in 2007 and the PhD degree in microwave technology from Xidian University, China in 2013. Currently, he is working with the Key Laboratory of Antennas and Microwave Technology at Xidian University as a professor. His research interests include electromagnetic compatibility, design of antennas, and microwave circuits.

WU Zengqiang received his BE degree and MS degree in microwave technology from Xidian University, China in 2015 and 2018, respectively. Currently, he is an RF engineer in ZTE Corporation. His research interests include microwave engineering design, modeling, and optimization.

GONG Hongwei joined ZTE Corporation as an RF&MW filter design director in 2015. He was in charge of all the RF filter design in ZTE and has made excellent progress in this domain. His research interests include electromagnetic compatibility, optimization and microwave device design.